Phys. Scr. **81** (2010) 015301 (8pp) doi:10.1088/0031-8949/81/01/015301

Spectroscopy of M-shell x-ray transitions in Zn-like through Co-like W

J Clementson[1], P Beiersdorfer, G V Brown and M F Gu[2]

Lawrence Livermore National Laboratory, Livermore, CA 94550, USA

E-mail: clementson@llnl.gov

Received 14 July 2009
Accepted for publication 13 November 2009
Published 24 December 2009
Online at stacks.iop.org/PhysScr/81/015301

Abstract
The M-shell x-ray emission of highly charged tungsten ions has been investigated at the Livermore electron beam ion trap facility. Using the SuperEBIT electron beam ion trap and a NASA x-ray calorimeter array, transitions connecting to levels of the ground configurations in the 1500–3600 eV spectral range of zinc-like W^{44+} through cobalt-like W^{47+} have been measured. The measured spectra are compared with theoretical line positions and emissivities calculated using the FAC code.

PACS numbers: 32.30.Rj, 31.30.J−, 52.70.La

1. Introduction

Tungsten is gaining interest in fusion engineering as a plasma-facing material in magnetic confinement devices, see e.g. [1–3]. Some present-day tokamaks are already operating with tungsten surfaces or are currently installing tungsten parts [4]. The ITER tokamak, now under construction in Cadarache, France, will have a tungsten divertor.

The use of tungsten in magnetic fusion experiments will introduce trace amounts of tungsten ions into the high-temperature, low-density plasmas. Tungsten ions that enter into a tokamak will not become fully stripped even in the hot core, resulting in strong x-ray emission over a wide range of temperatures. Provided the spectra are well understood, the tungsten ions can serve as diagnostics for plasma parameters [5, 6]. For instance, the ion temperatures of the ITER core plasmas will likely be measured using the Doppler broadening of L-shell tungsten lines [7].

Forty-six times ionized tungsten ions have 28 electrons arranged in a filled M-shell structure (unlike Ni I with a ground configuration of $3s^2 3p^6 3d^4_{3/2} 3d^4_{5/2} 4s^2$) and are therefore abundant over a large temperature range in high-temperature plasmas. This renders the nickel-like tungsten spectrum important for diagnostic purposes. The tungsten M-shell spectra of nickel-like and neighboring charge states have been extensively investigated, see for example [5, 8–29]. Further references can be found in the Kramida and Shirai review of atomic data for tungsten ions [30].

In recent years, Neill *et al* [13], Safronova *et al* [16, 17] and Ralchenko *et al* [20] have measured M-shell tungsten spectra on electron beam ion traps. Safronova *et al* and Ralchenko *et al* used x-ray calorimeter spectrometers for broadband spectral surveys. X-ray calorimeters (also known as quantum calorimeters or microcalorimeters) provide lower spectroscopic resolution than crystal spectrometers; however, the higher throughput and the very broad spectral coverage make these novel spectrometers very useful for the study of atomic spectra. Measurements of high-Z ions that have several transition bands particularly benefit from x-ray calorimeters. For instance, high charge states of Au were recently observed at the Livermore SuperEBIT, enabling line identifications and charge balance modeling [31]. In this paper, we report on the application of an x-ray calorimeter array at SuperEBIT to derive spectral line positions of M-shell x-ray transitions of W^{44+} through W^{47+}.

2. Experimental set-up

The measurements were carried out using the SuperEBIT electron beam ion trap at the Lawrence Livermore National Laboratory. SuperEBIT was operated in a low-energy configuration, making it similar to EBIT-I [32], at electron beam energies close to 3.3, 4.0 and 4.1 keV. These energies are of interest for the study of nickel-like tungsten, which is created from copper-like tungsten at 2414.1 eV and ionizes to cobalt-like at 4057 eV [33].

[1] Also at Department of Physics, Lund University, SE-221 00 Lund, Sweden.
[2] Present address: Space Sciences Laboratory, University of California, Berkeley, CA 94720, USA.

Table 1. Configuration state functions included in the structure calculations. $n = 4$, 5, 6 for Zn, Cu and Co, $n = 4$–8 for Ni; $n^* = 5, 6$; $l = 0, 1, \ldots, n-1$; $l^* = $ s, p.

Zn	Cu	Ni	Co
$3s^2 3p^6 3d^{10} 4l nl$	$3s^2 3p^6 3d^{10} nl$	$3s^2 3p^6 3d^{10}$	$3s^2 3p^6 3d^9$ $3s^2 3p^5 3d^{10}$ $3s 3p^6 3d^{10}$
$3s^2 3p^6 3d^9 4l 4l 4l$ $3s^2 3p^6 3d^9 4l^* 4l^* n^* l$	$3s^2 3p^6 3d^9 4l 4l$ $3s^2 3p^6 3d^9 4l^* n^* l$	$3s^2 3p^6 3d^9 nl$	$3s^2 3p^6 3d^8 nl$ $3s^2 3p^5 3d^9 nl$ $3s 3p^6 3d^9 nl$
$3s^2 3p^5 3d^{10} 4l 4l 4l$ $3s^2 3p^5 3d^{10} 4l^* 4l^* n^* l$	$3s^2 3p^5 3d^{10} 4l 4l$ $3s^2 3p^5 3d^{10} 4l^* n^* l$	$3s^2 3p^5 3d^{10} nl$	$3s^2 3p^5 3d^9 nl$ $3s^2 3p^4 3d^{10} nl$ $3s 3p^5 3d^{10} nl$
$3s 3p^6 3d^{10} 4l 4l 4l$ $3s 3p^6 3d^{10} 4l^* 4l^* n^* l$	$3s 3p^6 3d^{10} 4l 4l$ $3s 3p^6 3d^{10} 4l^* n^* l$	$3s 3p^6 3d^{10} nl$	$3s 3p^6 3d^9 nl$ $3s 3p^5 3d^{10} nl$ $3p^6 3d^{10} nl$

The tungsten ions were injected into the SuperEBIT trap using one of two methods: Metal Vapor Vacuum Arc (MeVVA) injection and sublimation injection. Most of the data were acquired using the faster sublimation injection. For this method, sublimation of tungsten hexacarbonyl, $W(CO)_6$, occurred in a vial attached to one of SuperEBIT's six radial vacuum ports. Once in a gaseous form, $W(CO)_6$ molecules freely entered the trap region through the port. As tungsten carbonyl molecules continuously fill the trap, the charge state distributions typically consist of several tungsten ions. Alternatively, the MeVVA injector discharges bunches of low charge state ions into the trap from a tungsten cathode, located at the top of SuperEBIT, once every trap cycle. As a result, the EBIT plasmas have a more peaked charge state distribution. Sodium metal was also sublimated and injected as a neutral gas, which, together with low-Z plasma impurities, provided reference spectra for energy calibration.

The x-ray emission was recorded with a NASA X-ray Spectrometer (XRS) x-ray calorimeter [34–36] developed at the Goddard Space Flight Center. The XRS spectrometer is a medium-resolution energy-dispersive instrument for soft and hard x-rays made up of an array of HgTe and Bi heat absorbers. For this measurement, 23 of the HgTe pixel elements were used. The resolution of 6.5 eV full-width at half-maximum equals a resolving power $E/\Delta E = 230$–550 for the spectral interval of interest. The data from the pixel elements were corrected for individual voltage drifts and then added together.

3. Calculations and spectral modeling

Transition energies of zinc-like through cobalt-like tungsten were calculated using the fully relativistic atomic physics package FAC v1.1.1 [37]. Keeping the K and L shells closed, energy levels and transition energies were calculated for the M and N shells. Table 1 lists the included configuration state functions.

Collisional-radiative models were constructed for the spectra of the four tungsten ions. The plasmas were modeled with electron beam energies of 3.3 and 4.1 keV at an electron density of 5×10^{11} cm^{-3}. Electron impact excitation and deexcitation were included as well as autoionization for the Cu- and Zn-like charge states. The calculated spectra for an excitation energy of 4.1 keV and line widths of 6.5 eV are shown in figure 1.

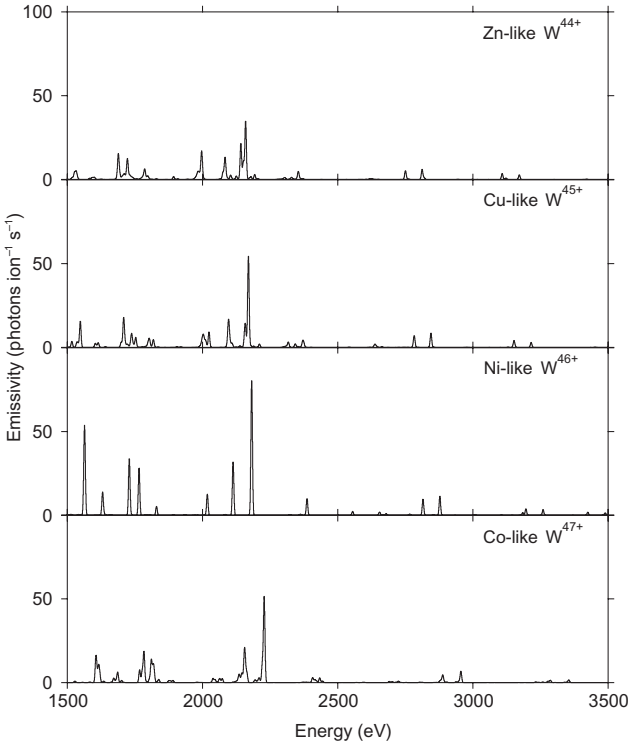

Figure 1. Calculated tungsten spectra at an excitation energy of 4.1 keV. The assumed line width is 6.5 eV.

4. Experimental tungsten spectra

The spectra analyzed comprise tungsten hexacarbonyl injection data obtained at beam energies close to 3.3, 4.0 and 4.1 keV, and MeVVA injection data obtained at an electron beam energy of 4.1 keV. The 4.1 keV carbonyl spectrum was energy calibrated with the $(3s^2 3p^6 3d^{10})_0$–$(3s^2 3p^6 3d^3_{3/2} 3d^6_{5/2} 4p_{1/2})_1$ Ni-like W line, which has been accurately measured at EBIT-I by Elliott *et al* [27], and with K-shell emission from low-Z elements (Na, Si, Cl, Ar and K) with transition energies calculated by Garcia and Mack [38], Drake [39] and Vainshtein and Safronova [40]. Ni-like W line positions determined from this spectrum were then used as reference lines in the other spectra. Conversion factors used were $hc = 12\,398.42$ Å eV $= 8065.5410$ eV cm.

The broadband XRS spectra are dominated by Ni-like W lines with upper levels of $n = 4$, 5, 6, 7 and 8. Lines from the lower charge states are often blended. Energies of the Co-like lines were derived from the 4.1 keV MeVVA spectrum, and the Cu- and Zn-like line positions were derived from 3.3 and 4.0 keV spectra. As far as a position of a given line was measured more than once, the results were averaged. An overview spectrum covering the 1–4 keV spectral band at a beam energy of 4.0 keV is shown in figure 2. The 3.3 keV spectrum, divided into three energy regions, is shown in figure 3, and the 4.1 keV spectrum, also divided, is shown in figure 4. The high-n transitions in Ni-like W were measured in the 4.1 keV spectrum and are shown in figure 5. This spectrum also shows lines from impurity ions.

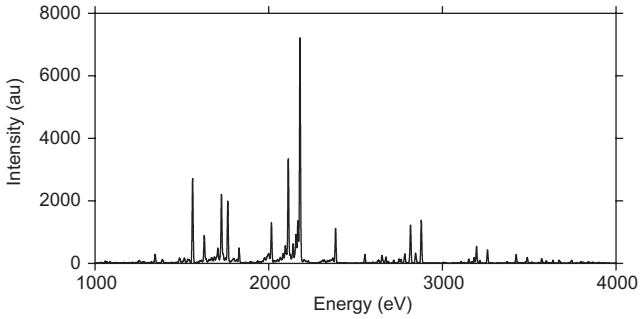

Figure 2. SuperEBIT XRS spectrum recorded at an electron beam energy of 4.0 keV.

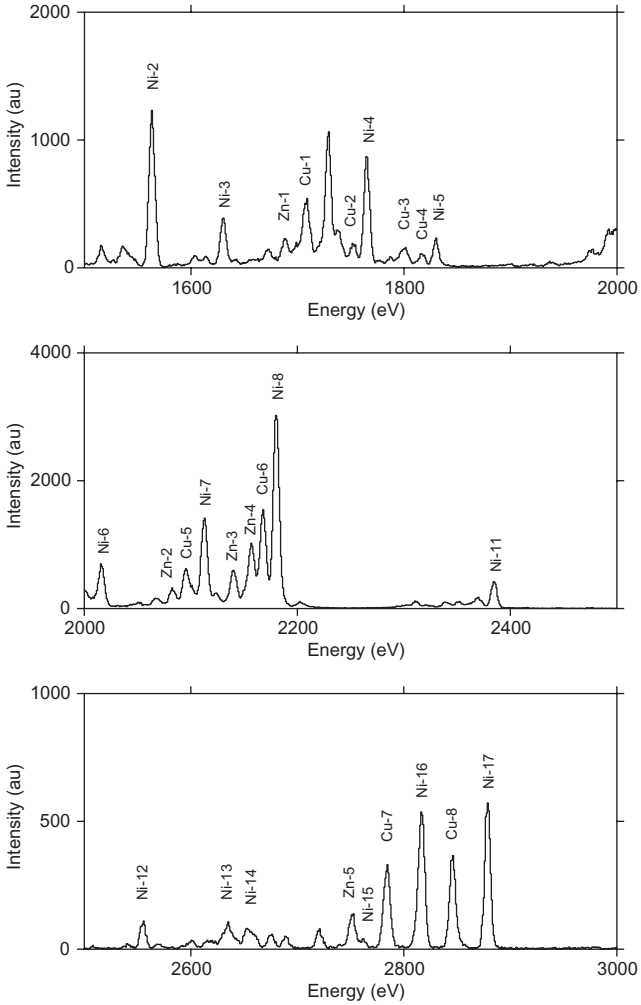

Figure 3. SuperEBIT XRS spectra recorded at an electron beam energy of 3.3 keV.

The measured lines are listed in tables 2–5 together with the theoretical line positions calculated using FAC. Most measured features have very good counting statistics and the spectroscopic accuracy is then limited by the calibration uncertainty, which varies from 0.3 to 0.5 eV. The total uncertainty of the line positions consists of the errors associated with the counting statistics and the energy scale added in quadrature. Only features that are dominated by transitions from one charge state are listed, and some features that are too broad or not fully resolved have been omitted. For the somewhat weaker or broader features the error bars have been doubled. The XRS is energy dispersive and measures

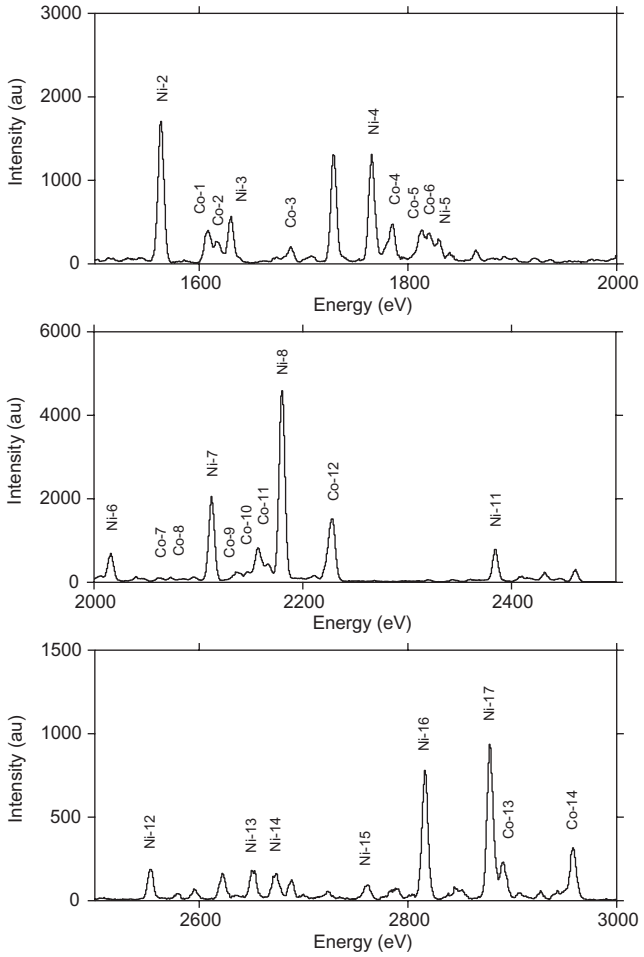

Figure 4. SuperEBIT XRS spectra recorded at an electron beam energy of 4.1 keV.

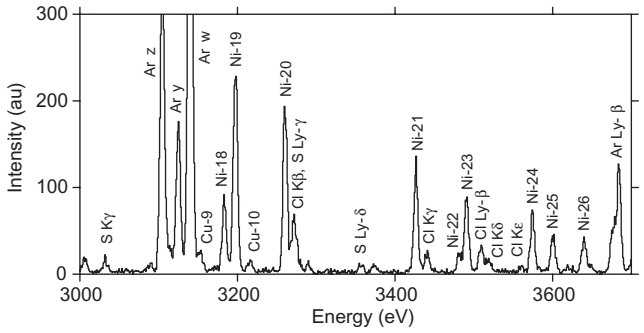

Figure 5. High-n transitions of Ni-like W^{46+} recorded at an electron beam energy of 4.1 keV.

photon energies, but corresponding wavelengths are also listed in the tables.

In the following, we discuss the results obtained for each of the four charge states of tungsten we have investigated.

4.1. Zn-like W^{44+}

The Zn-like lines are the weakest of the four charge states investigated. Seven lines are identified and listed in table 2. Line Zn-3 and one of the Zn-4 transitions are two-electron one-photon decays. Neill *et al* [13] observed these lines and assigned Zn-3 to be a line of Ga-like W and Zn-4 to be a resonance line from the $3d^3_{3/2}3d^6_{5/2}4s^24f_{5/2}$ configuration. As pointed out by Kramida

Table 2. Zn-like W^{44+} line positions measured with the NASA XRS spectrometer. Theoretical energies are from the present FAC calculations. [M]Mandelbaum *et al* [24], [N]Neill *et al* [13], [Ne]Neu *et al* [14], [T]Tragin *et al* [25], [Z1]Zigler *et al* [12]. *Comments on previous measurement are given in table 6.

Key	Transition lower level	upper level	Theory ΔE (eV)	Experiment ΔE (eV)	Experiment λ (Å)	Prev. Exp. λ (Å)
Zn-1	$(3s^23p^63d^{10}4s^2)_0$	$(3s^23p^63d^3_{3/2}3d^6_{5/2}4s^24p_{1/2})_1$	1688.1	1688.4(8)	7.3433(35)	7.332(3)[M*1] 7.34[Ne]
Zn-2	$(3s^23p^63d^{10}4s^2)_0$	$(3s^23p^63d^4_{3/2}3d^5_{5/2}4s^24f_{7/2})_1$	2082.6	2082.2(4)	5.9545(11)	
Zn-3	$(3s^23p^63d^{10}4s^2)_0$	$(3s^23p^63d^3_{3/2}3d^6_{5/2}4s_{1/2}4p_{3/2}4d_{3/2})_1$	2141.3	2139.7(8)	5.7945(22)	5.7928[N*2]
Zn-4	$(3s^23p^63d^{10}4s^2)_0$	$(3s^23p^63d^3_{3/2}3d^6_{5/2}4s_{1/2}4p_{3/2}4d_{5/2})_1$	2150.6	2156.4(16)	5.7496(42)	5.7676[N*3]
	$(3s^23p^63d^{10}4s^2)_0$	$(3s^23p^63d^3_{3/2}3d^6_{5/2}4s^24f_{5/2})_1$	2159.0			5.7471[N*4]
Zn-5	$(3s^23p^63d^{10}4s^2)_0$	$(3s^23p^63d^4_{3/2}3d^5_{5/2}4s^25f_{7/2})_1$	2750.2	2750.3(10)	4.5080(16)	4.507(2)[T*5] 4.509[Z1*5]
Zn-6	$(3s^23p^63d^{10}4s^2)_0$	$(3s^23p^63d^4_{3/2}3d^5_{5/2}4s^26f_{7/2})_1$	3107.9	3107.8(5)	3.9895(6)	3.990(5)[T] 3.988[Z1]
Zn-7	$(3s^23p^63d^{10}4s^2)_0$	$(3s^23p^63d^3_{3/2}3d^6_{5/2}4s^26f_{5/2})_1$	3171.0	3171.2(6)	3.9097(7)	3.909(5)[T] 3.909[Z1]

Table 3. Cu-like W^{45+} line positions measured with the NASA XRS spectrometer. Theoretical energies are from the present FAC calculations. [M]Mandelbaum *et al* [24], [N]Neill *et al* [13], [Ne]Neu *et al* [14], [T]Tragin *et al* [25], [Z1]Zigler *et al* [12]. *Comments on previous measurement are given in table 6.

Key	Transition lower level	upper level	Theory ΔE (eV)	Experiment ΔE (eV)	Experiment λ (Å)	Prev. Exp. λ (Å)
Cu-1	$(3s^23p^63d^{10}4s_{1/2})_{1/2}$	$(3s^23p^63d^3_{3/2}3d^6_{5/2}4s_{1/2}4p_{1/2})_{3/2}$	1707.3	1707.4(6)	7.2616(26)	7.262(3)[M] 7.26[Ne]
		$(3s^23p^63d^3_{3/2}3d^6_{5/2}4s_{1/2}4p_{1/2})_{1/2}$	1708.4			7.262(3)[M] 7.26[Ne]
Cu-2	$(3s^23p^63d^{10}4s_{1/2})_{1/2}$	$(3s^23p^63d^4_{3/2}3d^5_{5/2}4s_{1/2}4p_{3/2})_{3/2}$	1752.6	1751.9(8)	7.0771(32)	7.075(3)[M*6]
Cu-3	$(3s^23p^63d^{10}4s_{1/2})_{1/2}$	$(3s^23p^63d^3_{3/2}3d^6_{5/2}4s_{1/2}4p_{3/2})_{1/2}$	1797.6	1799.7(8)	6.8892(31)	6.896(3)[M]
		$(3s^23p^63d^3_{3/2}3d^6_{5/2}4s_{1/2}4p_{3/2})_{3/2}$	1801.4			6.884(3)[M]
	$(3s^23p^63d^{10}4p_{3/2})_{3/2}$	$(3s^23p^63d^3_{3/2}3d^6_{5/2}4s_{1/2}4d_{3/2})_{1/2}$	1803.8			
Cu-4	$(3s^23p^63d^{10}4s_{1/2})_{1/2}$	$(3s^23p^63d^3_{3/2}3d^6_{5/2}4s_{1/2}4p_{3/2})_{1/2}$	1817.2	1816.6(10)	6.8251(38)	6.827(3)[M]
	$(3s^23p^63d^{10}4p_{3/2})_{3/2}$	$(3s^23p^63d^3_{3/2}3d^6_{5/2}4p^2_{3/2})_{1/2}$	1818.4			6.816(3)[M*7]
Cu-5	$(3s^23p^63d^{10}4s_{1/2})_{1/2}$	$(3s^23p^63d^4_{3/2}3d^5_{5/2}4s_{1/2}4f_{7/2})_{3/2}$	2094.9	2094.8(5)	5.9187(14)	5.9127[N*8]
		$(3s^23p^63d^4_{3/2}3d^5_{5/2}4s_{1/2}4f_{7/2})_{1/2}$	2097.7			5.9127[N*8]
Cu-6	$(3s^23p^63d^{10}4s_{1/2})_{1/2}$	$(3s^23p^63d^3_{3/2}3d^6_{5/2}4s_{1/2}4f_{5/2})_{1/2}$	2168.6	2167.5(4)	5.7201(11)	5.7240[N*9]
		$(3s^23p^63d^3_{3/2}3d^6_{5/2}4s_{1/2}4f_{5/2})_{3/2}$	2169.8			5.7191[N*10]
Cu-7	$(3s^23p^63d^{10}4s_{1/2})_{1/2}$	$(3s^23p^63d^4_{3/2}3d^5_{5/2}4s_{1/2}5f_{7/2})_{1/2}$	2780.5	2783.0(8)	4.4551(13)	4.457(5)[T*11]
		$(3s^23p^63d^4_{3/2}3d^5_{5/2}4s_{1/2}5f_{7/2})_{3/2}$	2783.1			4.457(5)[T*11] 4.458[Z1*11]
Cu-8	$(3s^23p^63d^{10}4s_{1/2})_{1/2}$	$(3s^23p^63d^3_{3/2}3d^6_{5/2}4s_{1/2}5f_{5/2})_{1/2}$	2843.4	2845.1(4)	4.3578(6)	4.359(5)[T]
		$(3s^23p^63d^3_{3/2}3d^6_{5/2}4s_{1/2}5f_{5/2})_{3/2}$	2844.7			4.359(5)[T] 4.358[Z1]
Cu-9	$(3s^23p^63d^{10}4s_{1/2})_{1/2}$	$(3s^23p^63d^4_{3/2}3d^5_{5/2}4s_{1/2}6f_{7/2})_{1/2}$	3150.7	3152.5(5)	3.9329(6)	3.933(2)[T*12]
		$(3s^23p^63d^4_{3/2}3d^5_{5/2}4s_{1/2}6f_{7/2})_{3/2}$	3151.9			3.933(2)[T*12] 3.932[Z1]
Cu-10	$(3s^23p^63d^{10}4s_{1/2})_{1/2}$	$(3s^23p^63d^3_{3/2}3d^6_{5/2}4s_{1/2}6f_{5/2})_{3/2}$	3214.7	3215.8(5)	3.8555(6)	3.856(5)[T]
		$(3s^23p^63d^3_{3/2}3d^6_{5/2}4s_{1/2}6f_{5/2})_{1/2}$	3215.0			3.856(5)[T]

and Shirai [30], the two lines should be two-electron one-photon decays to the ground state. Kramida and Shirai suggest the lines to be from $3d^3_{3/2}3d^6_{5/2}4s_{1/2}4p_{3/2}4d_{3/2}$. Here, the FAC collisional-radiative model suggests that one of those lines instead is from $3d^3_{3/2}3d^6_{5/2}4s_{1/2}4p_{3/2}4d_{5/2}$. The calculations also suggest the Zn-4 line to be blended with two two-electron one-photon resonance decays in Cu-like W (from upper level $(3s^23p^63d^3_{3/2}3d^6_{5/2}4p_{3/2}4d_{3/2})_{3/2}$ at 2155.2 and 2158.3 eV). Zn-3 possibly blends with two Ga-like transitions ($3d^{10}4s^24p_{1/2}$–$3d^3_{3/2}3d^6_{5/2}4s^24p_{1/2}4f_{5/2}$), and Zn-5 possibly blends with a Ge-like line ($3d^{10}4s^24p^2_{1/2}$–$3d^3_{3/2}3d^6_{5/2}4s^24p^2_{1/2}5f_{5/2}$). The error bars of the energies associated with Zn-3, Zn-4 and Zn-5 have therefore been doubled.

4.2. Cu-like W^{45+}

Ten Cu-like features are reported in table 3. The lines are measured in the 3.3 and 4.0 keV spectra. Cu-8 is

Table 4. Ni-like W^{46+} line positions measured with the NASA XRS spectrometer. Theoretical energies are from the present FAC calculations. [B]Butzbach *et al* [43], [K]Klapisch *et al* [23], [M]Mandelbaum *et al* [24], [N]Neill *et al* [13], [Ne]Neu *et al* [14], [R]Ralchenko *et al* [20], [T]Tragin *et al* [25], [W]Wyart *et al* [44], [Z1]Zigler *et al* [12], [Z2]Zigler *et al* [11]. *Comments on previous measurement are given in table 6.

Key	Transition		Theory	Experiment		Prev. Exp.
	lower level	upper level	ΔE (eV)	ΔE (eV)	λ (Å)	λ (Å)
Ni-1	$(3s^23p^63d^3_{3/2}3d^6_{5/2}4p_{1/2})_1$	$(3s^23p^63d^3_{3/2}3d^6_{5/2}6d_{3/2})_0$	1487.0	1488.2(4)	8.3312(22)	8.326(11)[R]
Ni-2	$(3s^23p^63d^{10})_0$	$(3s^23p^63d^4_{3/2}3d^5_{5/2}4s_{1/2})_3$	1562.2	1562.9(3)	7.9330(15)	7.930(5)[R]
		$(3s^23p^63d^4_{3/2}3d^5_{5/2}4s_{1/2})_2$	1564.1			7.930(5)[R]
						7.93[Ne]
Ni-3	$(3s^23p^63d^{10})_0$	$(3s^23p^63d^3_{3/2}3d^6_{5/2}4s_{1/2})_2$	1630.0	1629.8(3)	7.6073(14)	7.607(6)[R]
Ni-4	$(3s^23p^63d^{10})_0$	$(3s^23p^63d^4_{3/2}3d^5_{5/2}4p_{3/2})_1$	1764.8	1764.6(3)	7.0262(12)	7.028(3)[M]
						7.030(4)[R]
						7.024(5)[Z2]
						7.028[K*13]
Ni-5	$(3s^23p^63d^{10})_0$	$(3s^23p^63d^3_{3/2}3d^6_{5/2}4p_{3/2})_1$	1829.4	1829.6(4)	6.7766(15)	6.779(3)[M]
						6.785(5)[R]
						6.775(5)[Z2]
						6.779[K*14]
Ni-6	$(3s^23p^63d^{10})_0$	$(3s^23p^2_{1/2}3p^3_{3/2}3d^{10}4s_{1/2})_1$	2017.4	2015.4(3)	6.1518(9)	6.155(4)[R]
						6.154(5)[Z2]
Ni-7	$(3s^23p^63d^{10})_0$	$(3s^23p^63d^4_{3/2}3d^5_{5/2}4f_{7/2})_1$	2112.6	2112.2(3)	5.8699(8)	5.867[N*15]
						5.872(2)[R]
						5.871(3)[Z2]
						5.8715(8)[B]
Ni-8	$(3s^23p^63d^{10})_0$	$(3s^23p^63d^3_{3/2}3d^6_{5/2}4f_{5/2})_1$	2181.4	2179.7(4)	5.6881(10)	5.690[N*16]
						5.691(2)[R]
						5.689(3)[Z2]
						5.6913(8)[B]
Ni-9	$(3s^23p^63d^{10})_0$	$(3s^23p_{1/2}3p^4_{3/2}3d^{10}4s_{1/2})_1$	2323.6	2320.3(6)	5.3435(14)	
Ni-10	$(3s^23p^63d^{10})_0$	$(3s^23p^2_{1/2}3p^3_{3/2}3d^{10}4d_{3/2})_1$	2361.8	2360.7(7)	5.2520(16)	5.2509[N*17]
						5.255(2)[T]
Ni-11	$(3s^23p^63d^{10})_0$	$(3s^23p^2_{1/2}3p^3_{3/2}3d^{10}4d_{5/2})_1$	2386.0	2384.2(4)	5.2002(9)	5.1963[N*18]
						5.203(2)[T]
						5.203(3)[R]
Ni-12	$(3s^23p^63d^{10})_0$	$(3s^23p^2_{1/2}3p^3_{3/2}3d^{10}4f_{7/2})_2$	2554.7	2553.0(4)	4.8564(8)	4.857(2)[T]
						4.857[W]
Ni-13	$(3s^23p^63d^{10})_0$	$(3s_{1/2}3p^63d^{10}4p_{1/2})_1$	2655.0	2651.3(4)	4.6764(7)	4.680(2)[T]
Ni-14	$(3s^23p^63d^{10})_0$	$(3s^23p_{1/2}3p^4_{3/2}3d^{10}4d_{3/2})_1$	2678.6	2673.7(6)	4.6372(10)	4.638(2)[T]
Ni-15	$(3s^23p^63d^{10})_0$	$(3s_{1/2}3p^63d^{10}4p_{3/2})_1$	2765.6	2760.7(5)	4.4910(8)	4.493(2)[T]
Ni-16	$(3s^23p^63d^{10})_0$	$(3s^23p^63d^4_{3/2}3d^5_{5/2}5f_{7/2})_1$	2814.9	2816.1(3)	4.4027(5)	4.406(2)[T]
						4.403(2)[R]
						4.409[Z1*19]
Ni-17	$(3s^23p^63d^{10})_0$	$(3s^23p^63d^3_{3/2}3d^6_{5/2}5f_{5/2})_1$	2877.3	2878.2(3)	4.3077(4)	4.309(2)[R]
						4.309(2)[T]
						4.311[Z1]
Ni-18	$(3s^23p^63d^{10})_0$	$(3s^23p^2_{1/2}3p^3_{3/2}3d^{10}5d_{5/2})_1$	3183.9	3182.7(4)	3.8956(5)	3.895(2)[T]
Ni-19	$(3s^23p^63d^{10})_0$	$(3s^23p^63d^4_{3/2}3d^5_{5/2}6f_{7/2})_1$	3195.5	3196.8(3)	3.8784(4)	3.877(2)[T]
						3.878(2)[R]
						3.879[Z1]
Ni-20	$(3s^23p^63d^{10})_0$	$(3s^23p^63d^3_{3/2}3d^6_{5/2}6f_{5/2})_1$	3258.9	3259.9(3)	3.8033(4)	3.803(2)[T]
						3.800(2)[R]
						3.803[Z1]
Ni-21	$(3s^23p^63d^{10})_0$	$(3s^23p^63d^4_{3/2}3d^5_{5/2}7f_{7/2})_1$	3424.4	3426.0(4)	3.6189(4)	3.618(2)[T]
Ni-22	$(3s^23p^63d^{10})_0$	$(3s^23p_{1/2}3p^4_{3/2}3d^{10}5d_{3/2})_1$	3482.7	3480.9(7)	3.5618(7)	3.551(2)[T]
Ni-23	$(3s^23p^63d^{10})_0$	$(3s^23p^63d^3_{3/2}3d^6_{5/2}7f_{5/2})_1$	3488.9	3490.2(4)	3.5524(4)	3.551(2)[T]
Ni-24	$(3s^23p^63d^{10})_0$	$(3s^23p^63d^4_{3/2}3d^5_{5/2}8f_{7/2})_1$	3572.5	3574.1(5)	3.4690(5)	3.469(2)[T]
Ni-25	$(3s^23p^63d^{10})_0$	$(3s^23p^2_{1/2}3p^3_{3/2}3d^{10}6d_{5/2})_1$	3600.9	3600.0(6)	3.4440(6)	3.445(2)[T*20]
Ni-26	$(3s^23p^63d^{10})_0$	$(3s^23p^63d^3_{3/2}3d^6_{5/2}8f_{5/2})_1$	3637.7	3639.5(6)	3.4066(6)	

Table 5. Co-like W^{47+} line positions measured with the NASA XRS spectrometer. Theoretical energies are from the present FAC calculations. [K] Klapisch *et al* [23], [M] Mandelbaum *et al* [24], [N] Neill *et al* [13], [T] Tragin *et al* [25]. *Comments on previous measurement are given in table 6.

Key	Transition lower level	upper level	Theory ΔE (eV)	Experiment ΔE (eV)	Experiment λ (Å)	Prev. Exp. λ (Å)
Co-1	$(3s^23p^63d^4_{3/2}3d^5_{5/2})_{5/2}$	$(3s^23p^63d^4_{3/2}3d^4_{5/2}4s_{1/2})_{9/2}$	1604.9	1607.6(4)	7.7124(19)	
		$(3s^23p^63d^4_{3/2}3d^4_{5/2}4s_{1/2})_{7/2}$	1608.0			
Co-2	$(3s^23p^63d^4_{3/2}3d^5_{5/2})_{5/2}$	$(3s^23p^63d^4_{3/2}3d^4_{5/2}4s_{1/2})_{5/2}$	1614.5	1617.2(10)	7.6666(47)	
		$(3s^23p^63d^4_{3/2}3d^4_{5/2}4s_{1/2})_{3/2}$	1616.0			
	$(3s^23p^2_{1/2}3p^3_{3/2}3d^{10})_{3/2}$	$(3s^23p^63d^3_{3/2}3d^5_{5/2}4d_{3/2})_{5/2}$	1618.2			
	$(3s^23p^63d^3_{3/2}3d^6_{5/2})_{3/2}$	$(3s^23p^63d^3_{3/2}3d^5_{5/2}4s_{1/2})_{7/2}$	1619.7			
Co-3	$(3s^23p^63d^4_{3/2}3d^5_{5/2})_{5/2}$	$(3s^23p^63d^3_{3/2}3d^5_{5/2}4s_{1/2})_{9/2}$	1685.9	1686.8(5)	7.3503(22)	
Co-4	$(3s^23p^63d^4_{3/2}3d^5_{5/2})_{5/2}$	$(3s^23p^63d^3_{3/2}3d^5_{5/2}4p_{1/2})_{7/2}$	1783.0	1783.8(8)	6.9506(31)	6.949(3)[M] 6.949[K]
		$(3s^23p^63d^3_{3/2}3d^5_{5/2}4p_{1/2})_{3/2}$	1783.1			6.949(3)[M] 6.949[K]
Co-5	$(3s^23p^63d^4_{3/2}3d^5_{5/2})_{5/2}$	$(3s^23p^63d^4_{3/2}3d^4_{5/2}4p_{3/2})_{7/2}$	1810.1	1812.4(8)	6.8409(30)	6.844(3)[M] 6.844[K]
		$(3s^23p^63d^4_{3/2}3d^4_{5/2}4p_{3/2})_{5/2}$	1810.5			6.844(3)[M] 6.844[K]
Co-6	$(3s^23p^63d^4_{3/2}3d^5_{5/2})_{5/2}$	$(3s^23p^63d^4_{3/2}3d^4_{5/2}4p_{3/2})_{5/2}$	1816.5	1820.6(8)	6.8101(30)	
		$(3s^23p^63d^4_{3/2}3d^4_{5/2}4p_{3/2})_{3/2}$	1820.3			6.806(3)[M*21] 6.806[K]
Co-7	$(3s^23p^63d^4_{3/2}3d^5_{5/2})_{5/2}$	$(3s^23p^2_{1/2}3p^3_{3/2}3d^4_{3/2}3d^5_{5/2}4s_{1/2})_{7/2}$	2060.8	2062.4(10)	6.0116(29)	
		$(3s^23p^2_{1/2}3p^3_{3/2}3d^4_{3/2}3d^5_{5/2}4s_{1/2})_{5/2}$	2064.3			
Co-8	$(3s^23p^63d^4_{3/2}3d^5_{5/2})_{5/2}$	$(3s^23p^2_{1/2}3p^3_{3/2}3d^4_{3/2}3d^5_{5/2}4s_{1/2})_{3/2}$	2072.7	2072.9(10)	5.9812(29)	
Co-9	$(3s^23p^63d^4_{3/2}3d^5_{5/2})_{5/2}$	$(3s^23p^63d^4_{3/2}3d^4_{5/2}4f_{5/2})_{5/2}$	2131.1	2137.1(10)	5.8015(27)	
		$(3s^23p^63d^4_{3/2}3d^4_{5/2}4f_{5/2})_{7/2}$	2133.6			
	$(3s^23p^2_{1/2}3p^3_{3/2}3d^{10})_{3/2}$	$(3s^23p^2_{1/2}3p^3_{3/2}3d^4_{3/2}3d^5_{5/2}4f_{5/2})_{1/2}$	2133.7			
		$(3s^23p^2_{1/2}3p^3_{3/2}3d^4_{3/2}3d^5_{5/2}4f_{5/2})_{5/2}$	2134.9			
	$(3s^23p^63d^4_{3/2}3d^5_{5/2})_{5/2}$	$(3s^23p^63d^4_{3/2}3d^4_{5/2}4f_{5/2})_{3/2}$	2135.6			
	$(3s^23p^2_{1/2}3p^3_{3/2}3d^{10})_{3/2}$	$(3s^23p^2_{1/2}3p^3_{3/2}3d^4_{3/2}3d^5_{5/2}4f_{5/2})_{3/2}$	2135.9			
	$(3s^23p^63d^4_{3/2}3d^5_{5/2})_{5/2}$	$(3s^23p^63d^4_{3/2}3d^4_{5/2}4f_{7/2})_{7/2}$	2137.7			
Co-10	$(3s^23p^63d^4_{3/2}3d^5_{5/2})_{5/2}$	$(3s^23p^63d^4_{3/2}3d^4_{5/2}4f_{7/2})_{5/2}$	2143.5	2146.9(10)	5.7750(27)	
		$(3s^23p^63d^4_{3/2}3d^4_{5/2}4f_{7/2})_{3/2}$	2145.1			5.7744[N*22]
Co-11	$(3s^23p^63d^4_{3/2}3d^5_{5/2})_{5/2}$	$(3s^23p^63d^4_{3/2}3d^4_{5/2}4f_{7/2})_{5/2}$	2153.5	2156.8(4)	5.7485(11)	5.7531[N*23]
		$(3s^23p^63d^4_{3/2}3d^4_{5/2}4f_{7/2})_{7/2}$	2155.4			5.7482[N*23]
		$(3s^23p^63d^4_{3/2}3d^4_{5/2}4f_{5/2})_{5/2}$	2158.0			
	$(3s^23p^63d^3_{3/2}3d^6_{5/2})_{3/2}$	$(3s^23p^63d^3_{3/2}3d^5_{5/2}4f_{7/2})_{5/2}$	2158.2			
Co-12	$(3s^23p^63d^4_{3/2}3d^5_{5/2})_{5/2}$	$(3s^23p^63d^3_{3/2}3d^5_{5/2}4f_{5/2})_{3/2}$	2220.8	2227.1(4)	5.5671(10)	5.5811[N*24]
		$(3s^23p^63d^3_{3/2}3d^5_{5/2}4f_{7/2})_{5/2}$	2225.0			5.5713[N*25]
		$(3s^23p^63d^3_{3/2}3d^5_{5/2}4f_{5/2})_{7/2}$	2227.5			5.5686[N*26]
		$(3s^23p^63d^3_{3/2}3d^5_{5/2}4f_{5/2})_{5/2}$	2228.4			5.5641[N*27]
Co-13	$(3s^23p^63d^4_{3/2}3d^5_{5/2})_{5/2}$	$(3s^23p^63d^4_{3/2}3d^4_{5/2}5f_{7/2})_{5/2}$	2887.0	2890.3(5)	4.2897(7)	4.289(2)[T*28]
		$(3s^23p^63d^4_{3/2}3d^4_{5/2}5f_{7/2})_{7/2}$	2888.5			4.289(2)[T*28]
Co-14	$(3s^23p^63d^4_{3/2}3d^5_{5/2})_{5/2}$	$(3s^23p^63d^3_{3/2}3d^5_{5/2}5f_{5/2})_{3/2}$	2954.0	2957.9(4)	4.1916(6)	4.192(2)[T*29]
		$(3s^23p^63d^3_{3/2}3d^5_{5/2}5f_{5/2})_{7/2}$	2955.3			4.192(2)[T*29]
		$(3s^23p^63d^3_{3/2}3d^5_{5/2}5f_{5/2})_{5/2}$	2955.5			4.192(2)[T*29]

possibly blended with a Ga-like resonance transition (from the $3d^3_{3/2}3d^6_{5/2}4p_{1/2}5f_{5/2}$ configuration), and hence, the error bar has been doubled.

4.3. Ni-like W^{46+}

Twenty-six nickel-like tungsten lines are identified and listed in table 4. They were mostly measured in the 4.1 keV spectrum, although many are average line positions from several spectra. Ni-1 is a weak N-shell transition, whereas the other observed lines are M-shell transitions. Ni-2 is made up of two energetically close dipole-forbidden transitions (cf [41]); a magnetic octupole and an electric quadrupole transition. These lines have recently been resolved with high-resolution crystal spectrometers [42]. The Ni-9 line position has been predicted by [11, 30], but has not previously been observed (here it is one of the weakest lines). A previously doubly classified line observed by Tragin *et al* [25] (also discussed in [30]), is resolved in this work, Ni-22 and Ni-23. As noted by Kramida and Shirai [30], the previously doubly classified line Ni-25 [25] should be dominated by the $(3s^23p^63d^{10})_0$–$(3s^23p^2_{1/2}3p^3_{3/2}3d^{10}6d_{5/2})_1$ transition.

4.4. Co-like W^{47+}

The features from cobalt-like tungsten were all measured in the 4.1 keV MeVVA spectrum and are listed in table 5. Co-like W has many transitions and only the dominating transitions

Table 6. Comments on the selection of the lines from previous work (PW) and earlier line assignments.

Key	Reference	Comment
*1	Mandelbaum *et al* [24]	Average λ of a broad feature. PW assigned several transitions to feature.
*2	Neill *et al* [13]	Average λ from five line lists. PW assigned the line to Ga-like W.
*3	Neill *et al* [13]	Average λ from three line lists. PW has different assignment.
*4	Neill *et al* [13]	Average λ from four line lists.
*5	Tragin *et al* [25] Zigler *et al* [12]	PW assigned feature blended with Ge-like W line.
*6	Mandelbaum *et al* [24]	PW assigned several transitions to feature.
*7	Mandelbaum *et al* [24]	PW assigned two transitions to feature.
*8	Neill *et al* [13]	Average λ from seven line lists.
*9	Neill *et al* [13]	Average λ from three line lists.
*10	Neill *et al* [13]	Average λ from seven line lists.
*11	Tragin *et al* [25] Zigler *et al* [12]	PW assigned feature blended with Ga-like W line.
*12	Tragin *et al* [25]	PW assigned two transitions to feature.
*13	Klapisch *et al* [23]	PW has no line assignment.
*14	Klapisch *et al* [23]	PW has no line assignment.
*15	Neill *et al* [13]	Average λ from ten line lists.
*16	Neill *et al* [13]	Average λ from ten line lists.
*17	Neill *et al* [13]	Average λ from five line lists.
*18	Neill *et al* [13]	Average λ from ten line lists.
*19	Zigler *et al* [12]	PW assigned two transitions to feature.
*20	Tragin *et al* [25]	PW assigned two transitions to feature.
*21	Mandelbaum *et al* [24]	PW assigned two transitions to feature.
*22	Neill *et al* [13]	Average λ from five line lists.
*23	Neill *et al* [13]	Average λ from five line lists.
*24	Neill *et al* [13]	Average λ from seven line lists.
*25	Neill *et al* [13]	Average λ from five line lists. PW has different assignment.
*26	Neill *et al* [13]	Average λ from eight line lists.
*27	Neill *et al* [13]	Average λ from six line lists.
*28	Tragin *et al* [25]	PW has no line assignment.
*29	Tragin *et al* [25]	PW has no line assignment.

in each feature are tabulated. The error bars for some of the weaker features have been doubled. Co-4 blends with two transitions at slightly lower energy giving the line a shoulder.

According to our FAC calculations, previous identifications for Co-12 [13, 30] are not correct. The 2225.0 eV transition is misidentified in [13] and the identifications for the 2225.0 eV and the 2228.4 eV transitions seem to be interchanged in [30].

5. Summary

The M-shell spectra of Zn-like through Co-like W ions have been measured using an x-ray calorimeter spectrometer at the SuperEBIT electron beam ion trap. Spectra were studied at excitation energies 3.3, 4.0 and 4.1 keV and show strong line emission in the 1500–3600 eV soft x-ray range. Line positions determined in our measurement are generally in good agreement with previous measurements when available and have significantly higher accuracies. Some of our lines have similar positions and error bars to those found earlier, but have been assigned to different transitions. This is likely to be due to the higher electron densities of the earlier experiments. A few lines, however, disagree with the work of Neill *et al* [13], although their measurements were performed at similar densities to ours. In addition, many lines have been presented which have been identified for the first time.

Relativistic atomic structure and collisional-radiative calculations have been performed using the FAC atomic physics code. Theoretical spectra are presented for Zn-like W^{44+} through Co-like W^{47+}. Very good agreement is established between calculated and observed spectra.

Acknowledgments

This work was performed under the auspices of the United States Department of Energy by Lawrence Livermore National Laboratory under contract DE-AC52-07NA-27344. The authors would like to acknowledge assistance with the experiment from Phil D'Antonio, Ed Magee, Dr Daniel Thorn, and Professor Elmar Träbert. Joel Clementson would like to thank Dr Hans Lundberg, Dr Sven Huldt and Professor Sune Svanberg for their support.

References

[1] Peacock N J, O'Mullane M G, Barnsley R and Tarbutt M 2008 Anticipated x-ray and VUV spectroscopic data from ITER with appropriate diagnostic implementation *Can. J. Phys.* **86** 277–84

[2] Skinner C H 2008 Applications of EBIT to magnetic fusion diagnostics *Can. J. Phys.* **86** 285–90

[3] Skinner C H 2009 Atomic physics in the quest for fusion energy and ITER *Phys. Scr.* T **134** 014022

[4] Neu R *et al* 2005 Tungsten: an option for divertor and main chamber plasma facing components in future fusion devices *Nucl. Fusion* **45** 209–18

[5] Biedermann C, Radtke R, Seidel R and Pütterich T 2009 Spectroscopy of highly charged tungsten ions relevant to fusion plasmas *Phys. Scr.* T **134** 014026

[6] Reader J 2009 Spectral data for fusion energy: from W to W *Phys. Scr.* T **134** 014023

[7] Beiersdorfer P *et al* 2010 *J. Phys. B: At. Mol. Phys.* submitted

[8] Dong C Z, Fritzsche S and Xie L Y 2003 Energy levels and transition probabilities for possible x-ray laser lines of highly charged Ni-like ions *J. Quant. Spectrosc. Radiat. Transfer* **76** 447–65

[9] Aggarwal K M, Norrington P H, Bell K L, Keenan F P, Pert G J and Rose S J 2000 Radiative rates for allowed transitions in Ni-like Nd, Sm, Eu, Ta, and W *At. Data Nucl. Data Tables* **74** 157–255

[10] Fournier K B 1998 Atomic data and spectral line intensities for highly ionized tungsten (Co-like W^{47+} to Rb-like W^{37+}) in a high-temperature, low-density plasma *At. Data Nucl. Data Tables* **68** 1–48

[11] Zigler A, Zmora H, Spector N, Klapisch M, Schwob J L and Bar-Shalom A 1980 Identification of spectra of Hf XLV, Ta XLVI, W XLVII, and Re XLVIII isoelectronic to Ni I in laser-produced plasmas *J. Opt. Soc. Am.* **70** 129–32

[12] Zigler A, Klapisch M and Mandelbaum P 1986 Interpretation of laser produced Au and W x-ray spectra in the 3 KeV range *Phys. Lett.* A **117** 31–5

[13] Neill P, Harris C, Safronova A S, Hamasha S, Hansen S, Safronova U I and Beiersdorfer P 2004 The study of x-ray *M*-shell spectra of W ions from the Lawrence Livermore National Laboratory electron beam ion trap *Can. J. Phys.* **82** 931–42

[14] Neu R, Fournier K B, Schlögl D and Rice J 1997 Observations of x-ray spectra from highly charged tungsten ions in tokamak plasmas *J. Phys. B: At. Mol. Opt. Phys.* **30** 5057–67

[15] Neu R, Fournier K B, Bolshukhin D and Dux R 2001 Spectral lines from highly charged tungsten ions in the soft-x-ray region for quantitative diagnostics of fusion plasmas *Phys. Scr.* T **92** 307–10

[16] Safronova A S *et al* 2008 The importance of EBIT data for z-pinch plasma diagnostics *Can. J. Phys.* **86** 267–76

[17] Shlyaptseva A, Fedin D, Hamasha S, Harris C, Kantsyrev V, Neill P, Ouart N and Safronova U I 2004 Development of M-shell x-ray spectroscopy and spectropolarimetry of z-pinch tungsten plasmas *Rev. Sci. Instrum.* **75** 3750–2

[18] Osborne G C, Safronova A S, Kantsyrev V L, Safronova U I, Yilmaz M F, Williamson K M, Shrestha I and Beiersdorfer P 2008 Diagnostic of charge balance of high-temperature tungsten plasmas using LLNL EBIT *Rev. Sci. Instrum.* **79** 10E308

[19] Loch S D, Pindzola M S, Ballance C P, Griffin C P, Whiteford A D and Pütterich T 2006 Modeling the spectral emission from tungsten in tokamaks *Spectral Line Shapes: 18th Int. Conf.* ed E Oks and M Pindzola (New York: AIP) **874** 233–241

[20] Ralchenko Y, Tan J N, Gillasy J D, Pomeroy J M and Silver E 2006 Accurate modeling of benchmark x-ray spectra from highly charged ions of tungsten *Phys. Rev.* A **74** 042614

[21] Ralchenko Y 2007 Density dependence of the forbidden lines in Ni-like tungsten *J. Phys. B: At. Mol. Opt. Phys.* **40** F175–F180

[22] Hamasha S M, Shlyaptseva A S and Safronova U I 2004 E1, E2, M1, and M2 transitions in the nickel isoelectronic sequence *Can. J. Phys.* **82** 331–56

[23] Klapisch M, Mandelbaum P, Barshalom A, Schwob J L, Zigler A and Jackel S 1981 Identification of 3d-4p transitions in Co-like W XLVIII and Tm XLIII and in Cu-like W XLVI and Tm XLI from laser-produced plasmas *J. Opt. Soc. Am.* **71** 1276–81

[24] Mandelbaum P, Klapisch M, Bar-Shalom A, Schwob J L and Zigler A 1983 Classification of x-ray spectra from laser produced plasmas of atoms from Tm to Pt in the range 6–9 Å *Phys. Scr.* **27** 39–53

[25] Tragin N, Geindre J P, Monier P and Gauthier J C 1988 Extended analysis of the x-ray spectra of laser-irradiated elements in the sequence from tantalum to lead *Phys. Scr.* **37** 72–82

[26] Burkhalter P G, Dozier C M and Nagel D J 1977 X-ray spectra from exploded-wire plasmas *Phys. Rev.* A **15** 700–17

[27] Elliott S R, Beiersdorfer P, MacGowan B J and Nilsen J 1995 Measurements of line overlap for resonant spoiling of x-ray lasing transitions in nickel-like tungsten *Phys. Rev.* A **52** 2689–92

[28] Pütterich T, Neu R, Dux R, Whiteford A D, O'Mullane M G and the ASDEX Upgrade Team 2008 Modelling of measured tungsten spectra from ASDEX upgrade and predictions for ITER *Plasma Phys. Control. Fusion* **50** 1–27

[29] Ballance C P and Griffin D C 2006 Relativistic radiatively damped R-matrix calculation of the electron-impact excitation of W^{46+} *J. Phys. B: At. Mol. Opt. Phys.* **39** 3617–28

[30] Kramida A E and Shirai T 2009 Energy levels and spectral lines of tungsten, W III through W LXXIV *At. Data Nucl. Data Tables* **95** 305–474

[31] Brown G V, Hansen S B, Träbert E, Beiersdorfer P, Widmann K, Chen H, Chung H K, Clementson J H T, Gu M F and Thorn D B 2008 Investigation of the $2p_{3/2}$–$3d_{5/2}$ line emission of Au^{53+}-Au^{69+} for diagnosing high energy density plasmas *Phys. Rev.* E **77** 066406

[32] Levine M A, Marrs R E, Henderson J R, Knapp M B and Schneider D A 1988 The electron beam ion trap: a new instrument for atomic physics measurements *Phys. Scr.* T **22** 157–63

[33] Kramida A E and Reader J 2006 Ionization energies of tungsten ions: W^{2+} through W^{71+} *At. Data Nucl. Data Tables* **92** 457–79

[34] Porter F S *et al* 2004 The Astro-E2 x-ray spectrometer/EBIT microcalorimeter x-ray spectrometer *Rev. Sci. Instrum.* **75** 3772–4

[35] Brown G V *et al* 2006 Laboratory astrophysics and atomic physics using the NASA/GSFC microcalorimeter spectrometers at the LLNL electron beam ion trap and radiation properties facility *Nucl. Instrum. Methods Phys. Res.* A **559** 623–5

[36] Porter F S *et al* 2008 The XRS microcalorimeter spectrometer at the Livermore electron beam ion trap *Can. J. Phys.* **86** 231–40

[37] Gu M F 2008 The flexible atomic code *Can. J. Phys.* **86** 675–89

[38] Garcia J D and Mack J E 1965 Energy level and line tables for one-electron atomic spectra *J. Opt. Soc. Am.* **55** 654–85

[39] Drake G W 1988 Theoretical energies for the $n = 1$ and 2 states of the helium isoelectronic sequence up to $Z = 100$ *Can. J. Phys.* **66** 586–611

[40] Vainshtein L A and Safronova U I 1985 Energy levels of He- and Li-like ions (states $1snl$, $1s^2nl$ with $n = 2$–5) *Phys. Scr.* **31** 519–32

[41] Beiersdorfer P, Osterheld A L, Scofield J, Wargelin B and Marrs R E 1991 Observation of magnetic octupole decay in atomic spectra *Phys. Rev. Lett.* **67** 2272–5

[42] Clementson J, Beiersdorfer P and Gu M F 2009 X-ray spectroscopy of E2 and M3 transitions in Ni-like W *Phys. Rev.* A submitted

[43] Butzbach R *et al* 1999 Spatially resolved high resolution spectroscopy of 4f-3d emission lines of Ni- and Co-like ions from Yb, Hf, Ta and W x-ray plasmas Paper presented at *X-ray Lasers Conf, Kyoto, Japan, 31 August–4 September 1998*, no. 159 (Institute of Physics) p 463

[44] Wyart J-F, Bauche-Arnoult C, Gauthier J-C, Geindre J-P, Monier P, Klapisch M, Bar-Shalom A and Cohn A 1986 Density-sensitive electric quadrupole decays in Ni-like ions observed in laser-produced plasmas *Phys. Rev.* A **34** 701